HAI YANG[1], WENCHANG ZHOU[1], LIPING YANG[2], JIYONG DENG[1],
QIAN HU[1], HONGQING WEI[1], CHAKTONG AU[1], BING YI[1]

$Ag^+/S_2O_8^{2-}$ SYSTEM FOR THE DEGRADATION OF AQUEOUS FLUTRIAFOL

The degradation of flutriafol in aqueous persulfate ($S_2O_8^{2-}$) system in the presence of selected transition metal ions was investigated. In the presence of Ag^+ or Fe^{2+}, flutriafol degradation occurs, whereas in the presence of Mn^{2+}, Co^{2+}, Ni^{2+}, Cu^{2+}, Zn^{2+} and Bi^{3+} ions, the degradation is less than 15%. The $Ag^+/S_2O_8^{2-}$ aqueous system being the most effective was adopted for experimental and theoretical investigations. It was confirmed that pH of 3.0 is the most suitable, and that both $^{\cdot}SO_4^-$ and $^{\cdot}OH^-$ radicals are the main active species to afford flutriafol degradation, with the former contributes more than the latter. To elucidate degradation mechanism, molecular orbital calculations were performed and reaction intermediates identified by GC/MS and HPLC/MS/MS analyses. Three degradation pathways are proposed that involve the cleavage of C–N and C–C bonds as a result of $^{\cdot}SO_4^-$ attack, as well as the formation of hydroxylated products due to $^{\cdot}OH$ radicals.

1. INTRODUCTION

As a triazole fungicide (Fig. 1), flutriafol is used for systemic foliar or seed treatment to control plant diseases through the inhabitation of C-14α-demethylase enzyme that participates in the biosynthesis of fungal sterols [1]. The compound has an important position in the global fungicide market because it can effectively control a vast number of diseases (e.g., cloud disease, leaf spot disease and rust disease) that affect a wide range of crops [2]. However, flutriafol is extremely persistent in soil, and being highly mobile, it is listed as a groundwater contaminant [3]. Despite not being used in the period of sampling, flutriafol at µg levels was detected in public water supply in England [4], Norway [5], Ireland [3] and other countries [6], indicating the persistence

_____

[1]College of Chemistry and Chemical Engineering, Hunan Institute of Engineering, Xiangtan 411104, P.R. China, corresponding author H. Yang, e-mail address: yanghai1001@163.com
[2]Shenzhen Academy of Environmental Sciences, Shenzhen 518001, P.R. China.

and accumulation of flutriafol in soil and ground water [7]. To understand the potential risk of secondary poisoning, it is meaningful to study the transformation of flutriafol in the environment. Flutriafol degrades through photolysis [8], oxidative [9], and biotransformation [10] processes. Nonetheless, the degradation rates are low under nutrient-limited conditions such as in subsurface soil or groundwater. For environment remediation, it is necessary to develop an effective method to determine the bioactivity, toxicity, metabolism, and degradation behavior of flutriafol in oxygen-depleted situations.
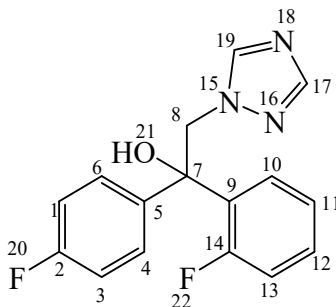

Fig. 1. Chemical structure of flutriafol with atoms labelled

Hydroxyl ($^{\bullet}OH$) and sulfate ($^{\bullet}SO_4^-$) radicals play important and decisive roles in the transformation of organic pollutants [11]. They both can initiate a series of chain reactions through which organic compounds are partially and/or fully decomposed [12]. Compared to $^{\bullet}OH$ ($E^0 = 2.80$ V vs. NHE, $t_{1/2} = 10^{-3}$ μs), $^{\bullet}SO_4^-$ ($E^0 = 2.43–2.80$ V vs. NHE, $t_{1/2} = 1–10$ μs) is similar in redox potential but more stable. There are $^{\bullet}SO_4^-$ radicals in ground waters originating from atmospheric SO_2, natural sulfur, and sulfur-based inorganic salts in industrial and household wastes [13].

Organic pollutants in water can be effectively degraded and transformed by $^{\bullet}SO_4^-$. However, the ecotoxicology, metabolic transformation and degradation products of flutriafol in the environment cannot be monitored easily because of the low concentration and interference from inorganic/organic matters. Zhang et al. [13] selected the sulfate radical-advanced oxidation process (SR-AOP) to study the transformation of pharmaceuticals, which is a promising approach for soil and groundwater remediation [14]. Among various oxidants available, persulfate ($S_2O_8^{2-}$) is the newest and least studied, but has received increasing attention [15]. Once $S_2O_8^{2-}$ is activated by heat, UV light, bases, transition metals, soil minerals, and radiolysis, $^{\bullet}SO_4^-$ radicals are formed [16]. In soil and groundwater, $^{\bullet}SO_4^-$ reacts with a wide variety of contaminants, generating reactive species such as $^{\bullet}OH$, HSO_5^- and H_2O_2 [17].

The $S_2O_8^{2-}$-based SR-AOP is superior in removing organic pollutants. Romero et al. [18] reported the degradation of diuron in a Fe(II)/$S_2O_8^{2-}$ system, and achieved complete oxidation of diuron in few minutes at 0.72 mmol/dm³ Fe(II) concentration. The same

Fe(II)/S$_2$O$_8^{2-}$ system was chosen by Zhou et al. [19] to remove diuron and As(III), and $^\bullet$OH and $^\bullet$SO$_4^-$ are key participants in the oxidation process in which As(III) is oxidized to As(V) via an electron-transfer step. Adopting the heat/S$_2$O$_8^{2-}$ system, Tan et al. [20] studied the degradation of diuron, and reported that $^\bullet$SO$_4^-$ was the principal agent responsible for its degradation. Furthermore, Mendez-Diaz et al. [21] examined the degradation efficiency of surfactant SDBS, and found that the UV/S$_2$O$_8^{2-}$ process was suitable. Despite these successful cases, the transformation mechanism of organic pollutants in S$_2$O$_8^{2-}$-based SR-AOP are not fully recognized. Moreover, it is a challenge to explore feasible methods for efficient generation of $^\bullet$SO$_4^-$ from S$_2$O$_8^{2-}$.

In the present study, the degradation of flutriafol in persulfate-based SR-AOPs was investigated theoretically and experimentally. First the S$_2$O$_8^{2-}$ activation efficiencies of selected transition metals were compared. Since silver was found to be the most efficient, the Ag$^+$/S$_2$O$_8^{2-}$ system was adopted to investigate the influence of chelating agents, pH values and substrate concentrations on flutriafol degradation. The related transformation mechanism was elucidated through molecular orbital calculations and identification of degradation intermediates.

2. MATERIALS AND METHODS

Materials. Flutriafol (≥99% purity) was purchased from the Hunan Research Institute of Chemical Industry. Sodium persulfate (Na$_2$S$_2$O$_8$, 99.1%) and ferrous sulfate heptahydrate (FeSO$_4$·7H$_2$O, 98%) were purchased from Sigma-Aldrich. Transition metal compounds (MnCl$_2$, Ni(NO$_3$)$_2$·6H$_2$O, ZnCl$_2$, Co(NO$_3$)$_2$·6H$_2$O, AgNO$_3$, Cu(NO$_3$)$_2$, Bi(NO$_3$)$_3$·5H$_2$O and FeCl$_2$) and the metal ion chelators: SCD (98%), Na$_2$S$_2$O$_3$·5H$_2$O (98%), DM (99%), and EDTA-Na$_2$ (98%), were supplied from Shanghai Sinopharm Chemical Reagent Co., Ltd., China. HPLC grade water was generated using a Millipore Milli-Q system in which the total organic carbon concentration was kept below 13 µg/dm^3 by constant illumination with a xenon arc lamp at 172 nm. Acetonitrile, menthol and ethanol (HPLC grade) were obtained from Sigma. The reagents were AR grade unless mentioned otherwise.

Experimental procedures. Homogeneous reactions were run at ambient temperature (25±2 °C) in a 250 cm^3 glass reactor wrapped with aluminum foil. A specific aliquot of 25–200 µmol/dm^3 flutriafol was transferred into the reactor, followed by the addition of a designated amount of Na$_2$S$_2$O$_8$ (0.1–10 mmol/dm^3) and transition metal salts (1.0 mmol/dm^3 MnCl$_2$, Ni(NO$_3$)$_2$·6H$_2$O, ZnCl$_2$, Co(NO$_3$)$_2$·6H$_2$O, AgNO$_3$, Cu(NO$_3$)$_2$, Bi(NO$_3$)$_3$·5H$_2$O and FeCl$_2$). The initial pH (1–11) of the solution was adjusted by using 0.1 mol/dm^3 HCl and 0.1 mol/dm^3 NaOH. The solution was constantly stirred with a magnetic stirrer. 1 cm^3 samples of the solution were taken at fixed time intervals, and quenched immediately by 1 cm^3 menthol, a quenching agent for $^\bullet$OH and $^\bullet$SO$_4^-$ radicals,

and then analyzed (after going through a 0.22 µm Millipore filter) by the HPLC and HPLC/MS/MS techniques. In the experiments of chelating agents, 1 mmol/dm^3 SCD, EDTA-Na$_2$, Na$_2$S$_2$O$_3$ and DM were added to simulate interference in the Ag$^+$/S$_2$O$_8^{2-}$ system (S$_2$O$_8^{2-}$ and Ag$^+$ concentration – 2.0 and 1.0 mmol/dm^3, respectively). Similarly, 0.1 mol/dm^3 ethanol and NaHCO$_3$ were added to Ag$^+$/S$_2$O$_8^{2-}$ system in the experiments of reactive oxygen species (ROS) scavengers, respectively. For GC/MS analysis, 50×3 cm^3 CH$_2$Cl$_2$ was added to the sample solution for extraction. The organic phase was collected, dried over Na$_2$SO$_4$ to desolventize at ambient temperature. The degradation efficiencies were calculated from the formula $((C_0 - C)/C_0 \times 100\%)$. Each batch of experiments was performed in triplicate, and the deviation was less than 5% in most of the cases.

Analytic methods. Flutriafol analysis was performed at 23 °C over a Cometro 6000 series HPLC using Kromasil C18 column (250×4.6 mm). The mobile phase was composed of 40% H$_2$O and 60% CH$_3$CN that was filtered with a Water Associates (Milford; MA, USA) 0.45 µm filter. The detection wavelength was 220 nm. The flow rate of the mobile phase was set at 1 cm^3/min.

Chromatographic analysis was carried out over a Shimadzu GCMS-QP2010 gas chromatograph/mass spectrometer equipped with a fused-silica capillary column coated with 5% diphenylmethylsilocane, viz. VF-5 (30 m×0.25 mm, 0.25 µm film thickness) from Varian. High-purity helium (99.9999%) at a constant flow rate of 1.5 cm^3/min was used as carrier gas. Employing an AOC-20i auto injector (275 °C), injections of 10^{-3} cm^3 were made in the splitless mode with 1.0 min purge-off time. The temperature program for analysis was: initial temperature 60 °C (held for 2 min), temperature raised (10 °C/min) to 200 °C (held for 1 min), and then to 275 °C and held at this temperature for 10 min. The GC was directly interfaced with the Shimadzu QP 2010 quadrupole mass spectrometer (250 °C interface temperature and 70 eV impact ionization). The transfer line was set at 275 °C, and the source at 200 °C. Positive fragment ions were analyzed over the 43–500 m/z mass range in SCAN mode. Unequivocal identification of target compounds was achieved through comparison with mass-spectral and special pesticide libraries (e.g., NIST, Wiley, PEST).

Degradation intermediates were analyzed using a HPLC/MS/MS equipment. HPLC separation was performed at 0.5 cm^3/min mobile phase (50% of H$_2$O and 50% of CH$_3$CN) within 30 min over a Shimadazu HPLC system equipped with a Kromasil C18 column (150×4.6 mm), and SIL-HT autosampler. With LC-10 AT vacuum pump and API 3000 mass analyzer, and through electrospray interface, MS and MS-MS analysis in positive ionization mode for full scan acquisition between m/z 50–450 were performed. The collision energy was varied according to measurement requirement, and the other parameters were set as follows: ESI 5.5 keV, source block and desolvation temperature 130 °C and 400 °C, respectively, desolvation and nebulizer gas (N$_2$) flow rate 6 dm^3/min, and argon (as collision gas) pressure 250 kPa.

Molecular orbital calculations were performed using Gaussian 03 program (Gaussian, Inc.) at the single determinant (HF/3-21) level. The optimal conformation having a minimum energy was obtained at the B3LYP/6-31G* level. The $(FED_{HOMO}^2 + FED_{LUMO}^2)$ and $2FED_{HOMO}^2$ values were acquired to predict the initial state of $^\cdot SO_4^-$ and $^\cdot OH$ interaction with the flutriafol molecule, respectively [22]. Also, the PCs were calculated based on NBO theory.

3. RESULTS AND DISSCUSSION

3.1. $S_2O_8^{2-}$ ACTIVATION BY TRANSITION METALS

The effect of Mn^{2+}, Ni^{2+}, Zn^{2+}, Co^{2+}, Ag^+, Cu^{2+}, Bi^{3+} and Fe^{2+} on persulfate activation was studied (Fig. 2). For the investigation, 1.0 mmol/dm^3 of metal cation was added, and NO_3^- or Cl^- was the counter anion.
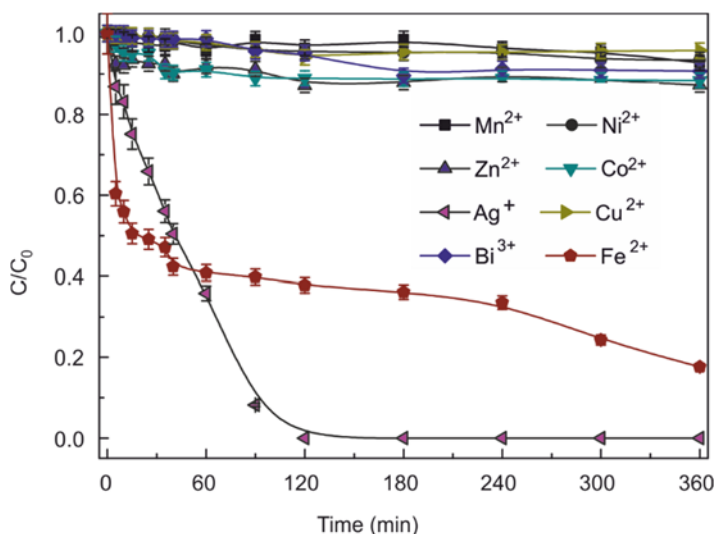

Fig. 2. Degradation efficiency of 100 μmol/dm^3 flutriafol
in the 1.0 mmol/dm^3 $S_2O_8^{2-}$ system activated by various transition metal ions

It was found that flutriafol (100 μmol/dm^3) degradation is 100% in 120 min with Ag^+ whereas it is less than 15% in 360 min with Mn^{2+}, Ni^{2+}, Zn^{2+}, Co^{2+}, Cu^{2+} and Bi^{3+}. With Fe^{2+}, flutriafol degradation is 82% in 360 min. Among the eight cases, flutriafol degradation is the worst with Bi^{3+} but best with Ag^+. The poor performance of Bi^{3+} is ascribed to its saturated electron configuration which is $5s^25p^65d^{10}6s^2$. With such electron configuration, Bi^{3+} is chemically inert. The electron configurations of Mn^{2+}, Fe^{2+}, Co^{2+}, Ni^{2+}, Cu^{2+} and Zn^{2+} are $3s^23p^63d^5$, $3s^23p^63d^6$, $3s^23p^63d^7$, $3s^23p^63d^8$, $3s^23p^63d^9$, and

$3s^2 3p^6 3d^{10}$, respectively. Despite the metal ions can accept electrons before attaining saturated electron configuration, they are poor in persulfate activation with Fe^{2+} being the only exception. It is because the Metal^{3+}/Metal^{2+} potentials of Mn^{2+}, Co^{2+}, Ni^{2+}, Cu^{2+} and Zn^{2+} are high while that of Fe^{2+} (Fe^{3+}/Fe^{2+}, $E^0 = 0.77$ V vs. NHE) is relatively low [22]. Interestingly, flutriafol degradation is the most efficient in the $Ag^+/S_2O_8^{2-}$ system. Ag^+ has an extra-nuclear electron configuration of $4s^2 4p^6 4d^{10}$ that allows the loss of an electron in the presence of a strong oxidant such as $S_2O_8^{2-}$. The standard Ag^{2+}/Ag^+ potential ($E^0 = 1.98$ V vs. NHE) is lower than the $S_2O_8^{2-}/SO_4^{2-}$ ($E^0 = 2.01$ V vs. NHE) and $SO_4^{2-}/{}^{\bullet}SO_4^-$ ($E^0 = 2.43-2.80$ V vs. NHE) potential, indicating that the transformation of Ag^+ to Ag^{2+} is feasible in the $Ag^+/S_2O_8^{2-}$ system.

3.2. SINGLE VARIABLE AT A TIME EXPERIMENTS IN $Ag^+/S_2O_8^{2-}$ SYSTEM

The flutriafol degradation ability of Ag^+ or $S_2O_8^{2-}$ is low. As shown in Fig. 3, there is only insignificant degradation of flutriafol over each of them. It is only in the presence of Ag^+ that a stronger oxidative ability of $S_2O_8^{2-}$ is released. We investigated the effect of Ag^+ concentration on the degradation of 100 µM/dm^3 flutriafol in the $Ag^+/S_2O_8^{2-}$ system by keeping $S_2O_8^{2-}$ constant at 2.0 mmol/dm^3. As shown in Fig. 4, an increase of Ag^+ concentration from 0.1 to 10 mmol/dm^3 results in gradual enhancement of degradation efficiency. And there is complete degradation of flutriafol in 10 min when Ag^+ concentration is 10 mmol/dm^3.

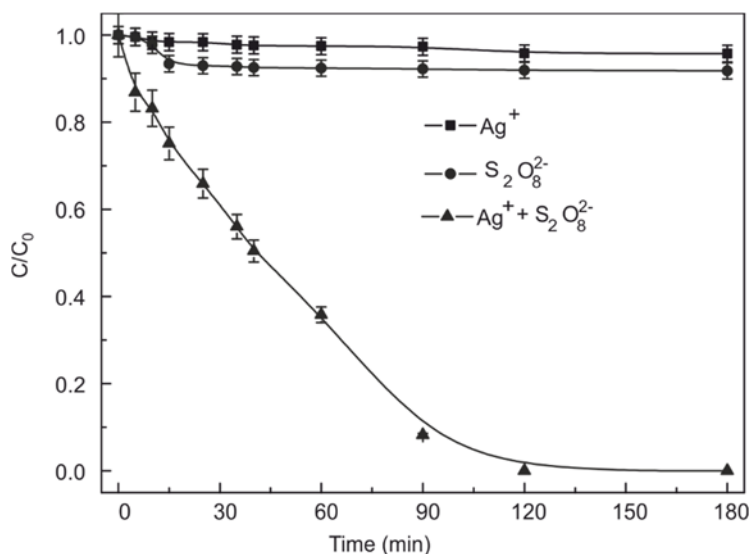Fig. 3. Degradation efficiency of 100 µmol/dm^3 flutriafol in
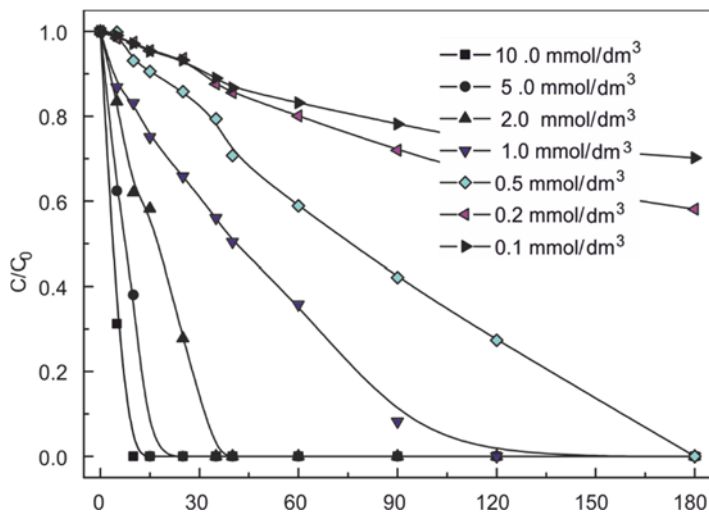1.0 mmol/dm^3 Ag^+, $S_2O_8^{2-}$ and $Ag^+/S_2O_8^{2-}$ systems

Fig. 4. Effect of Ag$^+$ concentration on the degradation efficiency of 100 μmol/dm^3 flutriafol
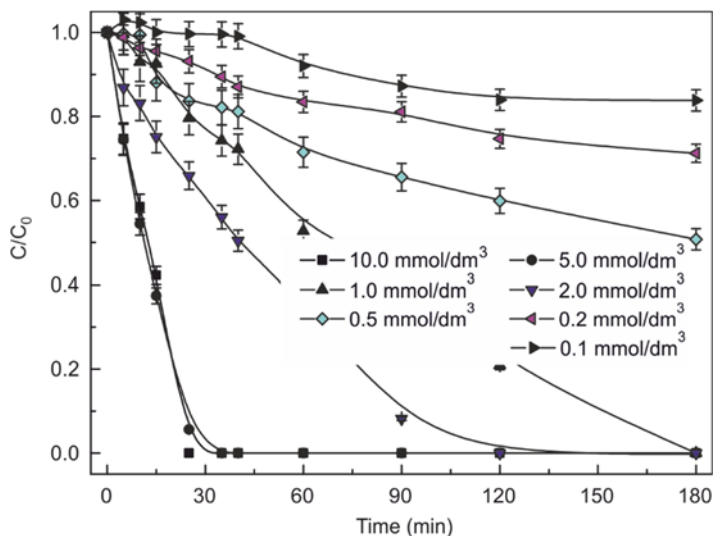in the Ag$^+$/S$_2$O$_8^{2-}$ system; the S$_2$O$_8^{2-}$ concentration – 2.0 mmol/dm^3

Fig. 5. Effect of S$_2$O$_8^{2-}$ concentration on the degradation efficiency of 100 μmol/dm^3 flutriafol
in the Ag$^+$/S$_2$O$_8^{2-}$ system; the Ag$^+$ concentration – 1.0 mmol/dm^3

On the other hand, when Ag$^+$ concentration is kept constant at 1.0 mmol/dm^3, there is increase of degradation efficiency when S$_2$O$_8^{2-}$ concentration is increased from 0.1 to 5.0 mmol/dm^3 (Fig. 5). And there was complete degradation of 100 μmol/dm^3 flutriafol in around 30 min when S$_2$O$_8^{2-}$ concentration was 5.0 mmol/dm^3. However, a further in-

crease of $S_2O_8^{2-}$ concentration to 10 mmol/dm^3 does not result in any increase of degradation efficiency. This might be due to the fact that too high $S_2O_8^{2-}$ concentration would result in other ROS being out-competed, leading to the stagnant of degradation efficiency [23].
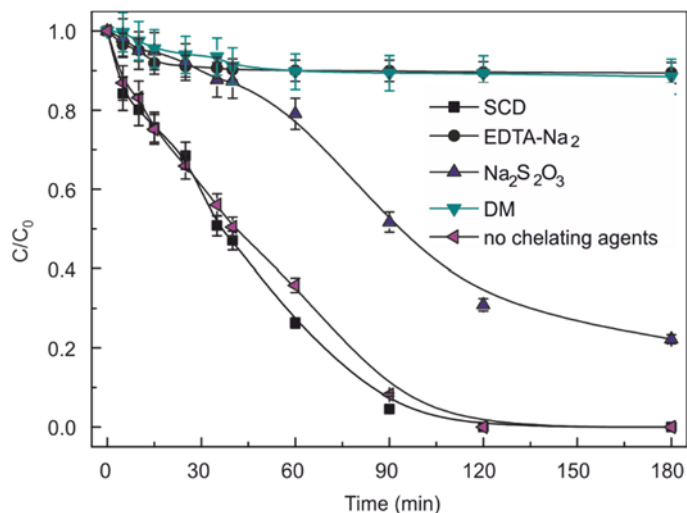

Fig. 6. Degradation efficiency of 100 µmol/dm^3 flutriafol in the Ag$^+$/$S_2O_8^{2-}$ system
with various chelating agents (1 mmol/dm^3),
$S_2O_8^{2-}$ and Ag$^+$ concentrations 2.0 and 1.0 mmol/dm^3, respectively
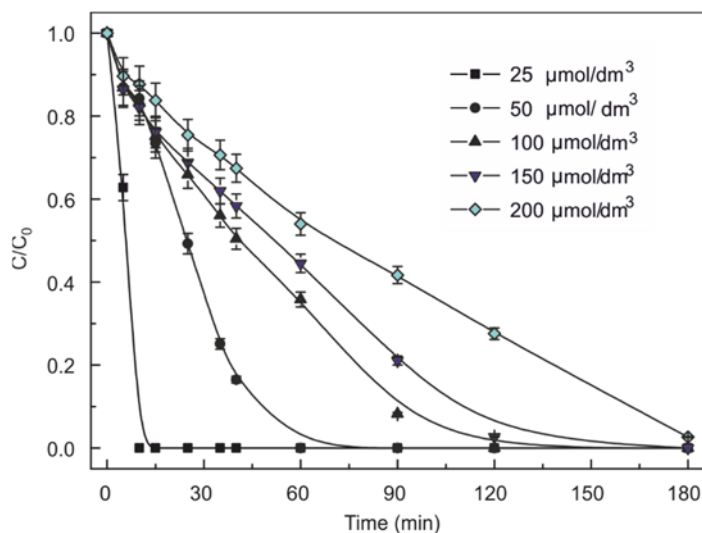
Fig. 7. Effect of flutriafol concentration (25–200 µmol/dm^3) on the degradation efficiency of flutriafol
in the Ag$^+$/$S_2O_8^{2-}$ system, $S_2O_8^{2-}$ and Ag$^+$ concentrations – 2.0 and 1.0 mmol/dm^3, respectively

The degradation of flutriafol was not affected by the addition of SCD, as seen in Fig. 6. However, with the addition of EDTA-Na$_2$ and DM, there is near complete suppression of flutriafol degradation, plausibly a result of their interaction with Ag$^+$, i.e., capturing Ag$^+$ through complex formation. With the capture of Ag$^+$, the activation of S$_2$O$_8^{2-}$ was denied. In the presence of Na$_2$S$_2$O$_3$, there was certain suppression of flutriafol degradation, which is a result of Ag$^+$ interaction with S$_2$O$_3^{2+}$, giving Ag$_2$S$_2$O$_3$ and Ag$_2$S (Eqs. (1) and (2)). The results confirm that once there is the capture of Ag$^+$ ions, the ability of the Ag$^+$/S$_2$O$_8^{2-}$ system for flutriafol degradation weakens.

$$S_2O_3^{2-} + 2Ag \rightarrow Ag_2S_2O_3 \downarrow \tag{1}$$

$$Ag_2S_2O_3 + H_2O \rightarrow Ag_2S + H_2SO_4 \downarrow \tag{2}$$

With the concentration of S$_2$O$_8^{2-}$ and Ag$^+$ fixed at 2 and 1 mmol/dm^3, respectively, we studied how the change of flutriafol concentration would influence the degradation efficiency (Fig. 7). From a flutriafol concentration of 25–200 μmol/dm^3, time for near complete degradation stretches from 10 to 180 min, indicating the amount of ROS in the Ag$^+$/S$_2$O$_8^{2-}$ system is limited.
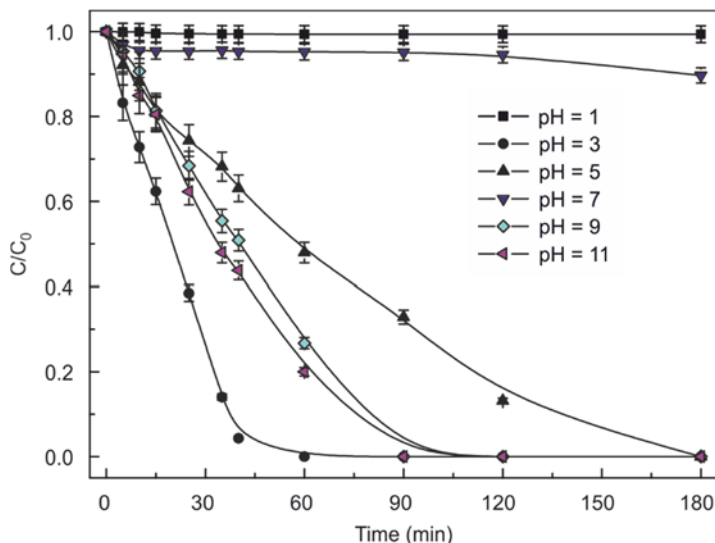
Fig. 8. Effect of pH on degradation efficiency of 100 μmol/dm^3 flutriafol in the Ag$^+$/S$_2$O$_8^{2-}$ system, S$_2$O$_8^{2-}$ and Ag$^+$ concentrations – 2.0 and 1.0 mmol/dm^3, respectively

pH of the solution is an important parameter affecting oxidative degradation of organic contaminants. We found that a change of initial pH value (from 1 to 11) affects

the $Ag^+/S_2O_8^{2-}$ system immensely (Fig. 8). When the solution is strongly acidic (pH 1) or neutral (pH 7), there is no degradation of flutriafol. It is only when the solution is weakly acidic (pH 3) or basic (pH 9 and 11) the degradation of flutriafol is observed. The lowest degradation efficiency at pH 1 is due to the removal of Ag^+ as a result of AgCl precipitation.

$$Ag^+ + Cl^- = AgCl\downarrow \tag{3}$$

With the removal of Ag^+, there is no activation of $S_2O_8^{2-}$. Nonetheless, we cannot give a proper explanation for the poor degradation efficiency at pH 7. Further experiments have to be performed to clarify such a phenomenon.

3.3. EFFECTS OF ROS AND PREDICTION OF ACTIVE SITES

To identify the dominating radical species in the $Ag^+/S_2O_8^{2-}$ system, quenching experiments were performed. Ethanol and $NaHCO_3$ were selected as quenching agents since the former is known to quench $^{\bullet}SO_4^-$ and $^{\bullet}OH$ while the latter $^{\bullet}SO_4^-$ [24, 25], and the results are shown in Fig. 9.
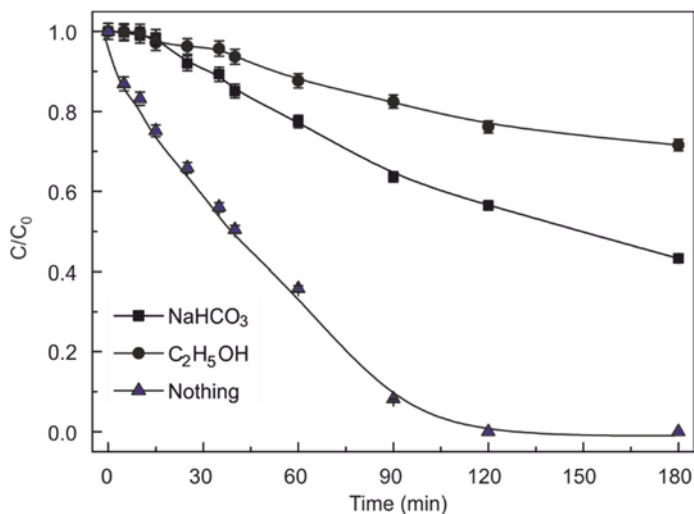
Fig. 9. Degradation curves of 100 μmol/dm³ flutriafol and flutriafol with scavengers (0.1 mol/dm³) in the $Ag^+/S_2O_8^{2-}$ system, $S_2O_8^{2-}$ and Ag^+ concentrations – to 2.0 and 1.0 mmol/dm³, respectively

With the addition of 0.1 mol/dm³ $NaHCO_3$ to the $Ag^+/S_2O_8^{2-}$ system the degradation efficiency decreases to 57%, suggesting that 43% degradation is due to $^{\bullet}SO_4^-$. When 0.1 mol/dm³ ethanol is used, the degradation efficiency decreases significantly to 28%, suggesting that 72% degradation is due to $^{\bullet}SO_4^-$ and $^{\bullet}OH$. A simple calculation shows

that the contribution of $^\bullet SO_4^-$ and $^\bullet OH$ is 43% and 29%, respectively, and the rest 28% is due to ROS such as peroxysulfate.

Point charges (PCs) and frontier electron densities (FEDs)
on atoms of flutriafol calculated by Gaussian 03 program
at the B3LYP/6-31G*

Atom label[a]	$2FED_{HOMO}^2$	$FED_{HOMO}^2 + FED_{LUMO}^2$	PCs
C_1	0.0896	0.0453	–0.0146
C_2	0.2006	0.3231	0.4056
C_3	0.0595	0.2017	–0.0150
C_4	0.0790	0.0423	0.0408
C_5	0.2815	0.3723	–0.0743
C_6	0.0509	0.2527	0.1068
C_7	0.0120	0.0136	0.2075
C_8	0.0345	0.0706	0.4266
C_9	0.1130	0.0928	–0.1281
C_{10}	0.0015	0.0512	0.0147
C_{11}	0.0782	0.0491	0.0031
C_{12}	0.0643	0.0499	0.0277
C_{13}	0.0047	0.0422	–0.0083
C_{14}	0.0743	0.0448	0.4784
N_{15}	0.0148	0.1148	–0.6673
N_{16}	0.0002	0.0631	–0.3743
C_{17}	0.0009	0.0312	0.5726
N_{18}	0.0019	0.0113	–0.6287
C_{19}	0.0007	0.0864	0.6985
F_{20}	0.0813	0.0616	–0.4105
O_{21}	0.0093	0.0182	–0.2683
F_{22}	0.0242	0.0126	–0.3931

[a]For the label of atoms refer to Fig. 1.

According to the frontier orbital theory, we looked into the nature of the active sites in the interaction of the flutriafol molecule with ROS. It is known that the locations with higher $FED_{HOMO}^2 + FED_{LUMO}^2$ values show higher tendency to interact with radicals, while those with higher $2FED_{HOMO}^2$ values are likely to lose electrons in oxidation reaction [26]. As shown in Table 1, the C_2, C_3, C_5 and C_6 of flutriafol show high $FED_{HOMO}^2 + FED_{LUMO}^2$ values of 0.4457, 0.3438, 0.4632 and 0.2527, respectively. The two benzene rings are different in reaction activity. The F atom at the *para*-position activates the benzene ring while that at the *ortho* position deactivates the benzene ring, resulting in the former being more reactive towards radical interaction. On the other hand, C_2, C_5 and C_9 show higher $2FED_{HOMO}^2$ values, indicating that these atoms of the benzene rings

are likely to lose electrons and get involved in oxidation reaction. As for C_2 and C_5, reactivity is low due to steric effect. It is hence reckoned that C_9 was the predicted position for oxidation reaction at the initial stage. Furthermore, the PC values show that C_2, C_8, C_{14}, C_{17} and C_{19} are positive while the heteroatoms N, O and F atoms are negative. Accordingly, the carbon atoms in the triazole ring and those connected with the F atoms have tendency to react with radicals, while the heteroatoms of the triazole ring are likely to react with H^+ and Ag^+.

3.4. INVESTIGATION OF DEGRADATION INTERMEDIATES AND TRANSFORMATION MECHANISM

By means of GC/MS and HPLC/MS/MS analysis we investigated the degradation intermediates and the transformation mechanism, and the TIC chromatograms of GC/MS and HPLC/MS/MS are presented in Figs. 10 and 11, respectively.
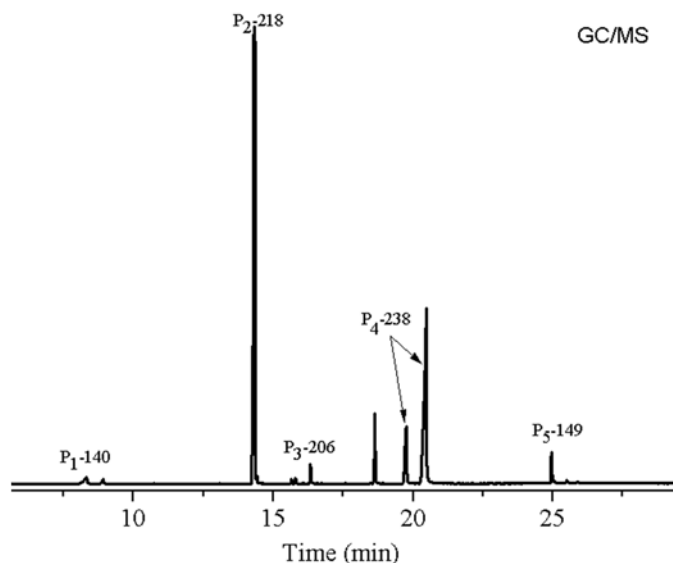

Fig. 10. TIC chromatogram from GC/MS

From Fig. 10, one can see five degradation intermediates, viz. P_1-140, P_2-218, P_3-206, P_4-238 and P_5-149. A search in the mass-spectral and special pesticide libraries revealed that P_1-140, P_2-218, and P_3-206 are 4-fluorobenzoic acid, (2-fluorophenyl) (4-fluorophenyl) methanone, and 1-(4-fluorophenyl)-2- (1H-1,2,4-triazol-1-yl) ethanone, respectively. And P_4-238 is the dihydroxylated products of P_3-206. The intermediate P_4-238 has two structural isomers, and it is not possible to distinguish the two based on the acquired data. Despite a thorough search, we failed to identify the structure

of P$_5$-149, and it is not possible to deduce a reasonable structure based on its MS fragments.
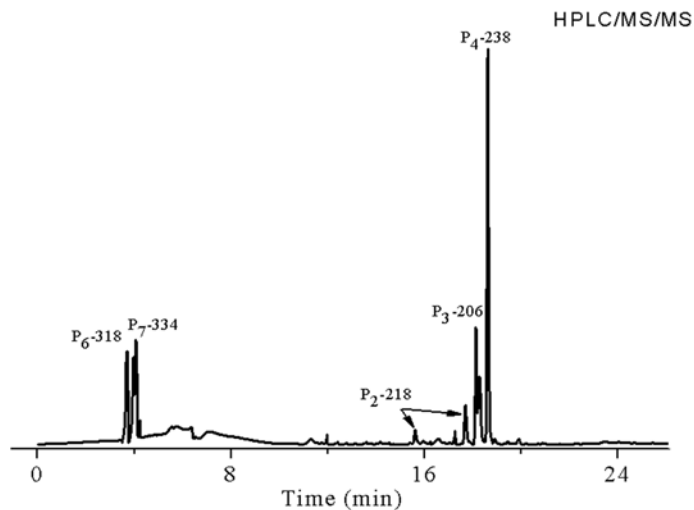
Fig. 11. TIC chromatogram from HPLC/MS/MS
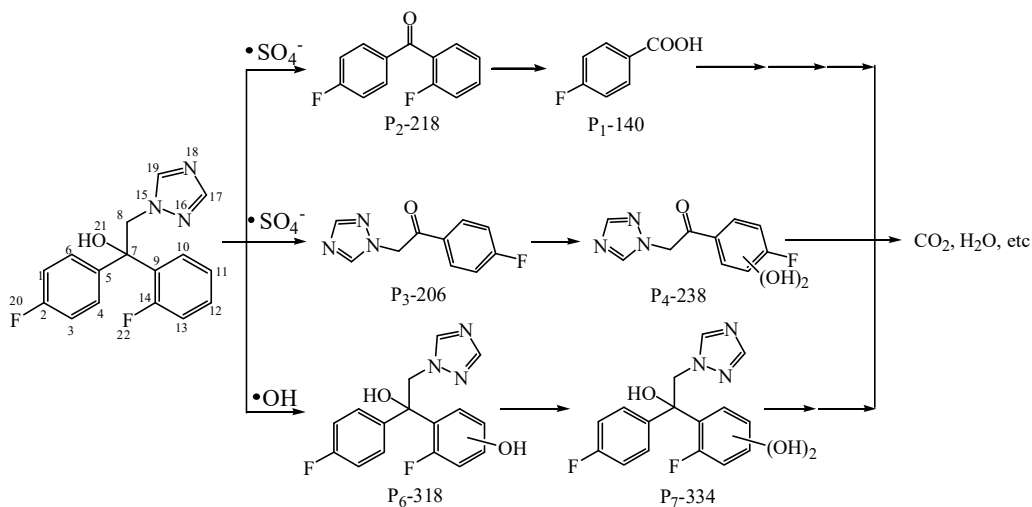
Fig. 12. Proposed transformation pathways of flutriafol in the $Ag^+/S_2O_8^{2-}$ system

In the HPLC/MS/MS analyzed (Fig. 11), the intermediates P$_2$-218, P$_3$-206 and P$_4$-238 are also found. Additionally, there are P$_6$-318 and P$_7$-334 that are ascribable to mono- and dihydroylated flutriafol, respectively. The hydroxylation products were reported before by Ghauch [27]. It is noted that P$_7$-334 is more polar than P$_6$-318, in agreement

with the fact that the former is a di-hydroylated product while the latter mono-hydroy-lated product of flutriafol.

Based on the degradation intermediates and the contribution of ROS, three degradation pathways are proposed as illustrated in Fig. 12. There is the $^{\bullet}SO_4^-$ attack toward the carbon atom (C8) connected to the tertiary alcohol, and 4-fluorobenzoic acid (P_1-140) and (2-fluorophenyl) (4-fluorophenyl) methanone (P_2-218) are produced as a result of C–N bond cleavage. On the other hand, the C–C bond (C_7–C_9) of tertiary alcohol is broken also due to $^{\bullet}SO_4^-$ attack to give 1-(4-fluorophenyl)-2-(1H-1,2,4-triazol-1-yl) ethanone (P_3-206) and its dihydroxylated products (P_4-238). Furthermore, $^{\bullet}OH$ reacts with the flutriafol molecule to give the monohydroxylated and dihydroxylated products.

3.5. ENVIRONMENTAL IMPLICATION

Based on the above results, the $Ag^+/S_2O_8^{2-}$ system can be used as an in situ oxidation method to remove flutriafol in waste-water treatment. However, attention has to be paid for the optimization of reaction parameters such as pH values and Ag^+ and $S_2O_8^{2-}$ concentrations. The results of the present studies provide insights into the transformation and degradation of flutriafol under the influence of $^{\bullet}SO_4^-$ and $^{\bullet}OH$. If the degradation intermediates were toxic, undesired ill effects would be resulted. It is hence essential to determine whether it is a necessity to achieve complete mineralization of degradation intermediates during the oxidation process. With the degradation pathways clarified and the intermediates identified, it is possible to examine the toxicity of the overall degradation process and have better understanding on its suitability in environment protection.

3. CONCLUSIONS

Flutriafol can be degraded efficiently in the $Ag^+/S_2O_8^{2-}$ system by $^{\bullet}SO_4^-$ which is generated when $S_2O_8^{2-}$ is activated by Ag^+. It was observed that an increase in the concentration of either Ag^+ or $S_2O_8^{2-}$ in the system results in enhancement of flutriafol degradation efficiency. Also, a decrease of flutriafol concentration results in increase of degradation rate. Furthermore, the results of kinetics studies indicate that chelating agents, EDTA-Na$_2$, Na$_2$S$_2$O$_3$ and dextrose monohydrate (DM), have negative effect on the performance of the $Ag^+/S_2O_8^{2-}$ system due to their ability in capturing Ag^+. And the best degradation efficiency of flutriafol is observed at pH 3.0. Both $^{\bullet}SO_4^-$ and $^{\bullet}OH$ radicals are involved in the degradation, with $^{\bullet}SO_4^-$ contributing more. With the identification of degradation intermediates by GC/MS and HPLC/MS/MS, three degradation pathways that involve the cleavage of C–N and C–C bonds and hydroxylation of the parent compound are proposed. Comparing the oxidation ability of $^{\bullet}SO_4^-$ and $^{\bullet}OH$, the

cleavage of the C–N and C–C bond is a result of $^{\bullet}SO_4^-$ attack, while the hydroxylation reactions are due to $^{\bullet}OH$. With the degradation pathways clarified, it is envisaged that the toxic effects of the degradation intermediates can be investigated and documented.

REFERENCES

[1] WHITE P.M., POTTER T.L., CULBREATH A.K., *Fungicide dissipation and impact on metolachlor aerobic soil degradation and soil microbial dynamics*, Sci. Total Environ., 2010, 408 (6), 1393.

[2] ZHANG Q., HUA X.D., SHI H.Y., LIU J.S., TIAN M.M., WANG M.H., *Enantioselective bioactivity, acute toxicity and dissipation in vegetables of the chiral triazole fungicide flutriafol*, J. Hazard. Mater., 2015, 28, 465.

[3] YU P.Z., JIA C.H., SONG W.C., LIU F.M., *Dissipation and residues of flutriafol in wheat and soil under field conditions*, B, Environ. Contam. Tox., 2012, 89 (5), 1040.

[4] MAVROEIDI V.I., SHAW M.W., *Sensitivity distributions and cross-resistance patterns of Mycosphaerella graminicola to fluquinconazole, prochloraz and azoxystrobin over a period of 9 years*, Crop. Prot., 2005, 24 (3), 259.

[5] HERMANSON M.H., ISAKSSON E.H., TEIXEIRA C., MUIR D.C.G., COMPHER K.M., LI Y.F., IGARASHI I., KAMIYAMA K., *Current-use and legacy pesticide history in the Austfonna ice cap, Svalbard, Norway*, Environ. Sci. Technol., 2005, 39 (21), 8163.

[6] CASARA K.P., VECCHIATO A.B., LOURENCETTI C., PINTO A.A., DORES E.F.G.C., *Environmental dynamics of pesticides in the drainage area of the Sao Lourenco River Headwaters, Mato Grosso State, Brazil*, J. Brazil. Chem. Soc., 2012, 23 (9), 1719.

[7] MUNIER-LAMY C., BORDE O., *Effect of a triazole fungicide on the cellulose decomposition by the soil microflora*, Chemosphere, 2000, 41 (7), 1029.

[8] MUIR D.C., TEIXEIRA C., WANIA F., *Empirical and modeling evidence of regional atmospheric transport of current-use pesticides*, Environ. Toxicol. Chem., 2004, 23 (10), 2421.

[9] GILBERT-LOPEZ B., GARCIA-REYES J.F., MOLINA-DIAZ A., *Determination of fungicide residues in baby food by liquid chromatography-ion trap tandem mass spectrometry*, Food Chem., 2012, 135 (2), 780.

[10] ZHANG Q., HUA X., YANG Y., YIN W., TIAN M., SHI H., WANG M., *Stereoselective degradation of flutriafol and tebuconazole in grape*, Environ. Sci. Pollut. Res. Int., 2015, 22 (6), 4350.

[11] YANG H., WEI H.Q., HU L.T., LIU H.J., YANG L.P., AU C.T., YI B., *Mechanism for the photocatalytic transformation of s-triazine herbicides by center dot OH radicals over TiO2*, Chem. Eng. J., 2016, 300, 209.

[12] YANG H., AN T., LI G., SONG W., COOPER W.J., LUO H., GUO X., *Photocatalytic degradation kinetics and mechanism of environmental pharmaceuticals in aqueous suspension of TiO2. A case of β-blockers*, J. Hazard. Mater., 2010, 179, 834.

[13] ZHANG R., SUN P., BOYER T.H., ZHAO L., HUANG C.H., *Degradation of pharmaceuticals and metabolite in synthetic human urine by UV, UV/H2O2, and UV/PDS*, Environ. Sci. Technol., 2015, 49 (5), 3056.

[14] LUTZE H.V., KERLIN N., SCHMIDT T.C., *Sulfate radical-based water treatment in presence of chloride: formation of chlorate, inter-conversion of sulfate radicals into hydroxyl radicals and influence of bicarbonate*, Water Res., 2015, 72, 349.

[15] YANG Y., PIGNATELLO J.J., MA J., MITCH W.A., *Comparison of halide impacts on the efficiency of contaminant degradation by sulfate and hydroxyl radical-based advanced oxidation processes (AOPs)*, Environ. Sci. Technol., 2014, 48 (4), 2344.

[16] OH W.D., LUA S.K., DONG Z., LIM T.T., *Performance of magnetic activated carbon composite as peroxymonosulfate activator and regenerable adsorbent via sulfate radical-mediated oxidation processes*, J. Hazard. Mater., 2015, 2, 841.

[17] ANIPSITAKIS G.P., DIONYSIOU D.D., *Radical generation by the interaction of transition metals with common oxidants*, Environ. Sci. Technol., 2004, 38 (13), 3705.

[18] ROMERO A., SANTOS A., VICENTE F., GONZALEZ C., *Diuron abatement using activated persulphate. Effect of pH, Fe(II) and oxidant dosage*, Chem. Eng. J., 2010, 162 (1), 257.

[19] ZHOU L., ZHENG W., JIA Y., ZHANG J., ZENG C., ZHANG Y., WANG Q., YANG X., *Ferrous-activated persulfate oxidation of arsenic(III) and diuron inaquatic system*, J. Hazard. Mater., 2013, 263, 422.

[20] TAN C.Q., GAO N.Y., DENG Y., AN N., DENG J., *Heat-activated persulfate oxidation of diuron in water*, Chem. Eng. J., 2012, 203, 294.

[21] MENDEZ-DIAZ J., SANCHEZ-POLO M., RIVERA-UTRILLA J., CANONICA S., VON GUNTEN U., *Advanced oxidation of the surfactant SDBS by means of hydroxyl and sulphate radicals*, Chem. Eng. J., 2010, 163 (3), 300.

[22] ZOU J., MA J., CHEN L., LI X., GUAN Y., XIE P., PAN C., *Rapid acceleration of ferrous iron/peroxymonosulfate oxidation of organic pollutants by promoting Fe(III)/Fe(II) cycle with hydroxylamine*, Environ. Sci. Technol., 2013, 47 (20), 11685.

[23] JI Y., FERRONATO C., SALVADOR A., YANG X., CHOVELON J.M., *Degradation of ciprofloxacin and sulfamethoxazole by ferrous-activated persulfate. Implications for remediation of groundwater contaminated by antibiotics*, Sci. Total Environ., 2014, 47, 2800.

[24] ZENG J., YANG H., LIU H., YI X., YANG L., YI B., *Common characteristic assessments of transformation mechanism for substituted phenylurea herbicides by reactive oxygen species (ROSs) during photocatalytic process*, Chem. Eng. J., 2015, 273, 519.

[25] YANG H., LIU H., HU Z., LIANG J., PANG H., YI B., *Consideration on degradation kinetics and mechanism of thiamethoxam by reactive oxidative species (ROSs) during photocatalytic process*, Chem. Eng. J., 2014, 245 (1), 24.

[26] YANG H., YANG L., HU Z., LIU H., PANG H., YI B., *General transformation law of chlorinated acetanilide herbicides by reactive oxidative species (ROSs) during photocatalytic process*, J. Water Process. Eng., 2015, 8, e66.

[27] GHAUCH A., *Rapid removal of flutriafol in water by zero-valent iron powder*, Chemosphere, 2008, 7, 1816.